

Determination of Deformation Mode in AZ61 Magnesium Alloy by Texture Simulations

Bartosz Sułkowski

*AGH-University of Science and Technology,
Faculty of Non-Ferrous Metals
Kraków, Poland*

Motivation

Increasing demand for Mg alloys e.g: automotive and transport industry,

New applications of Mg alloys - magnesium alloys products have been found to be excellent candidates for hydrogen storage or even for medical applications especially if the material is processed by severe plastic deformation

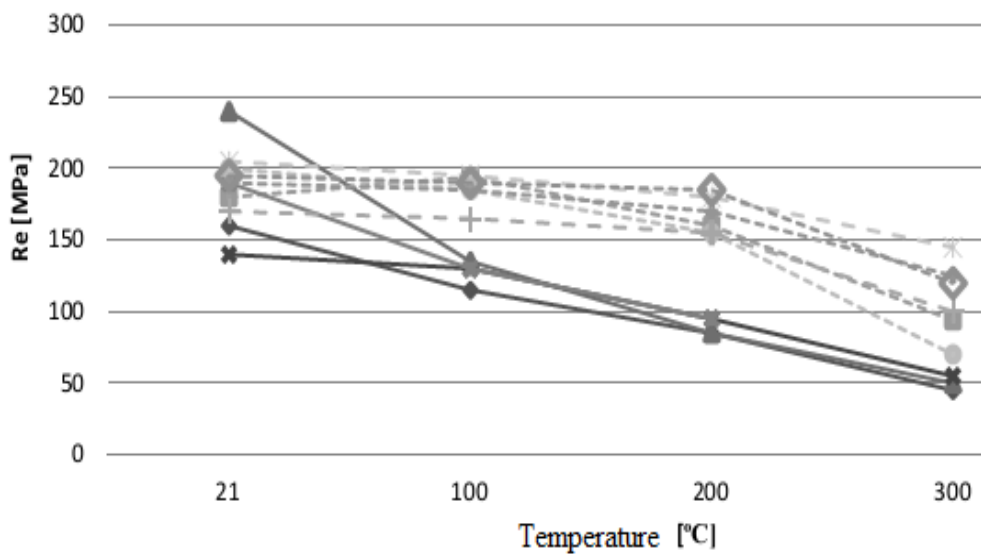
The plastic deformation of magnesium alloys is rather problematic due to the strong anisotropy of hexagonal structure – formation of strong basal texture during e.g. rolling

The ductility of magnesium alloys can be enhanced by means of weakening basal texture in many different ways:

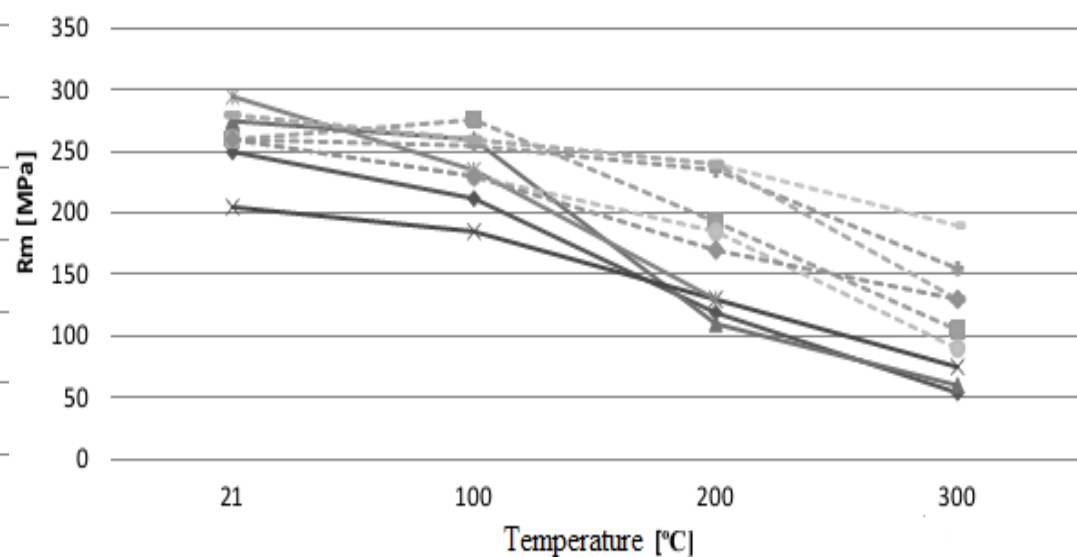
- changing of the rolling direction
- introducing shear component of deformation e.g. in differential speed rolling processing (DSR)
- dynamic recrystallization (DRX)
- DRX + massive twinning during rolling at very high strain rates ($\geq 10^1 \text{ s}^{-1}$)

	21°C			100°C			200°C			300°C		
Stop	Re	Rm	A[%]	Re	Rm	A[%]	Re	Rm	A[%]	Re	Rm	A[%]
AZ31	160	250	6	115	212	31	85	119	77	45	54	94
AZ61	180	260	7	194	276	26	160	193	75	94	105	90
AZ91	240	275	5	135	260	19	85	110	73	50	60	87
ZE41	140	205	5	130	185	8	95	130	29	55	75	43
ZE63	190	295	7	130	235	-	95	130	-	-	-	-
EV31	170	280	5	165	260	-	155	240	-	100	130	-
EQ21	195	260	4	190	230	10	185	170	16	120	130	10
QE22	200	260	4	185	230	12	155	185	20	70	90	59
WE43	190	260	7	185	255	-	170	235		125	155	-
WE54	205	280	4	195	260	8	185	240	11	145	190	15

An effect of temperature on yield point



An effect of temperature on tensile strength

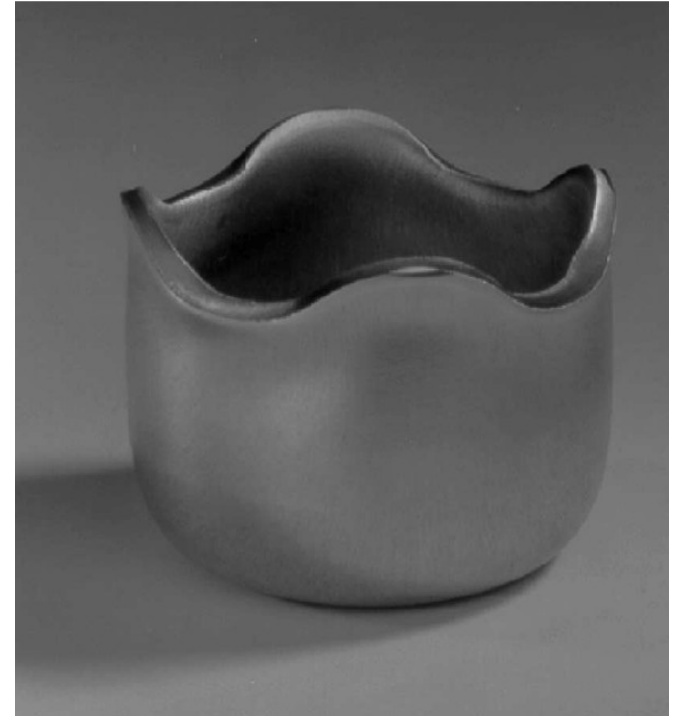
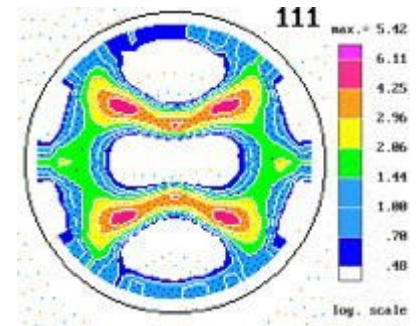
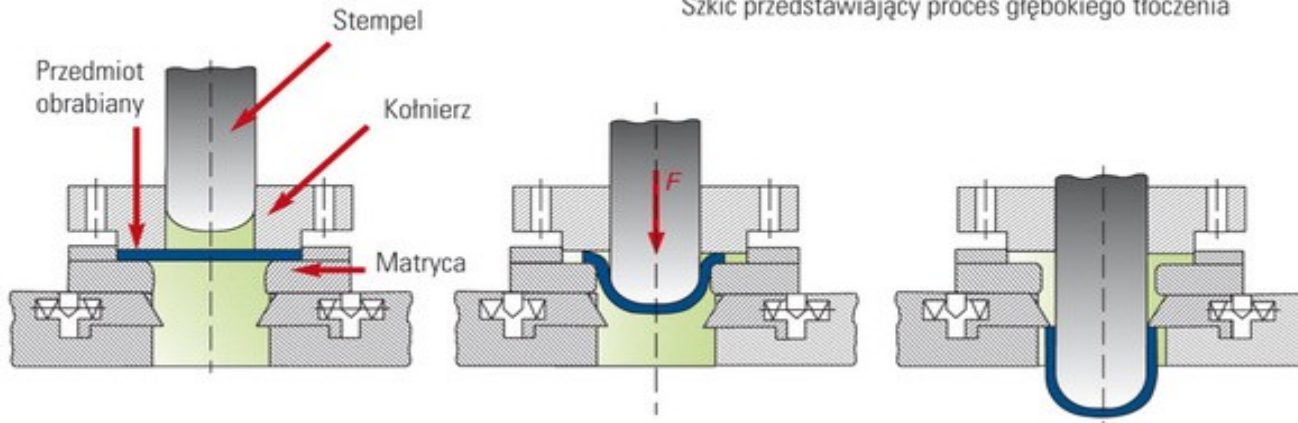


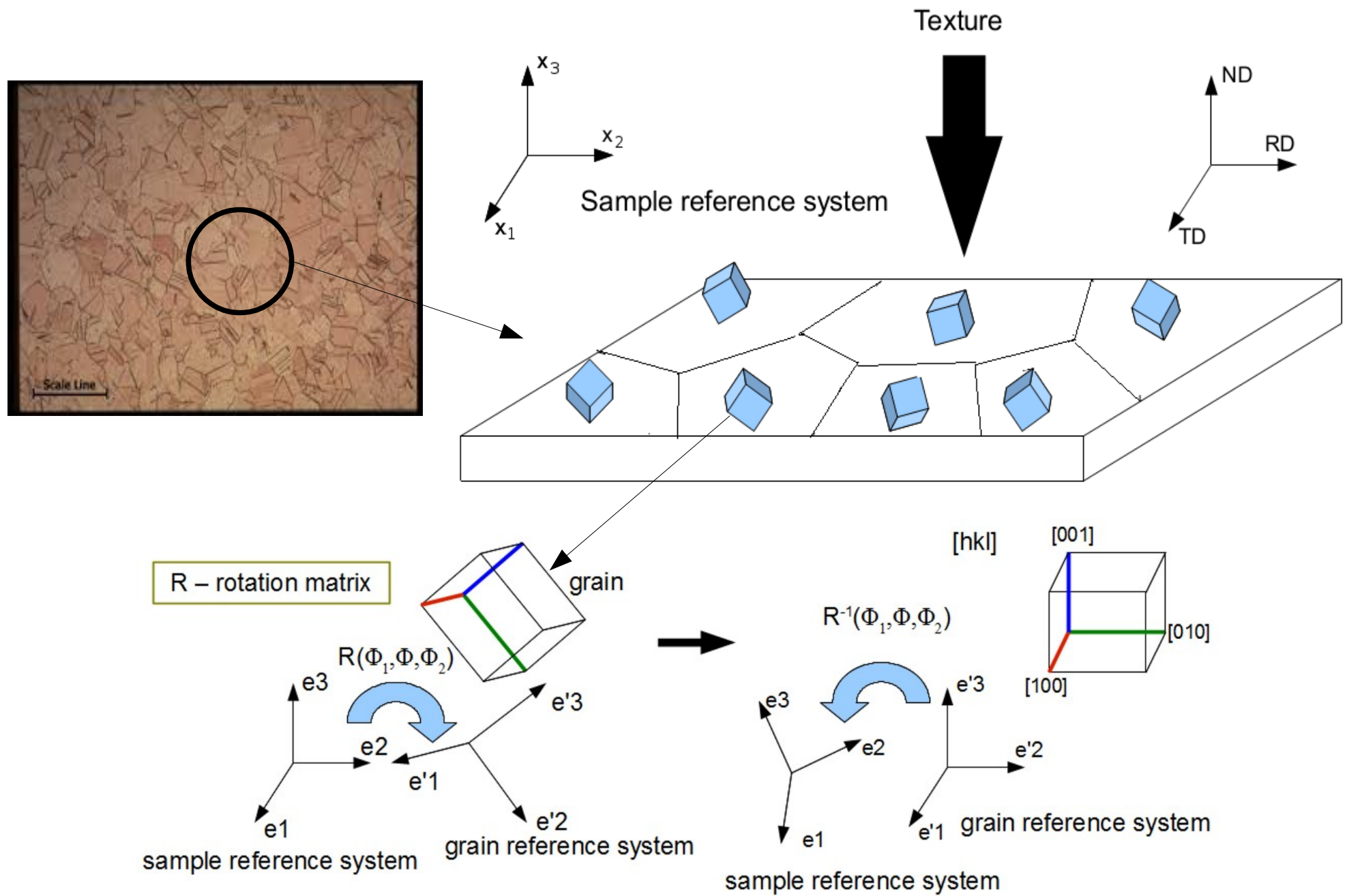
—◆— AZ31 -■- AZ61 —▲— AZ91 —×— ZE41 —*— ZE63
 -●- QE22 -◆- WE43 *— WE54 +— EV31 -◆- EQ21

—◆— AZ31 -■- AZ61 —▲— AZ91 —×— ZE41 —*— ZE63
 -●- QE22 -◆- WE43 *— WE54 +— EV31 -◆- EQ21

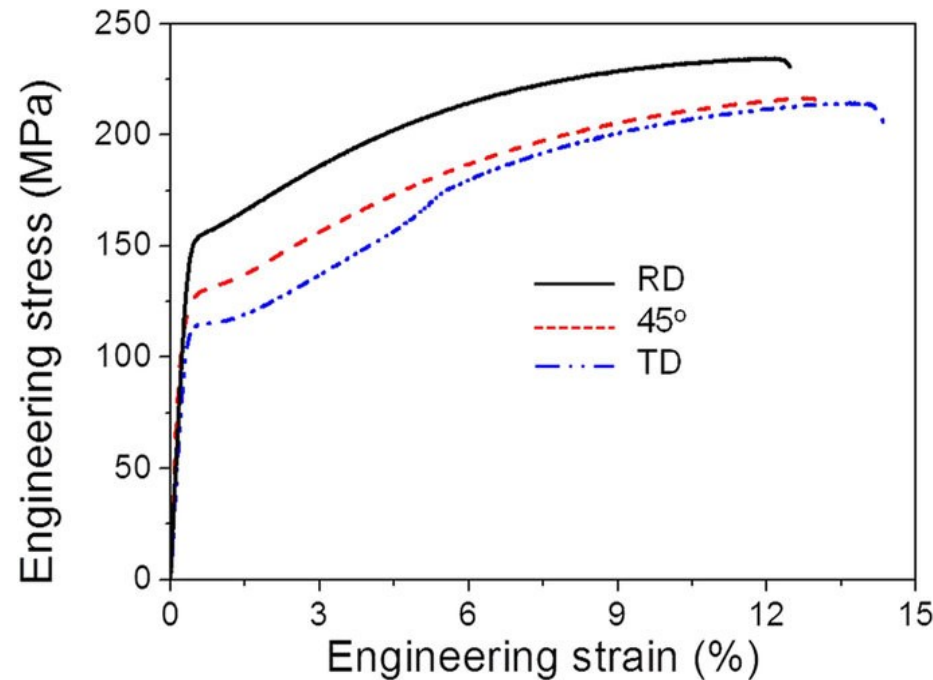
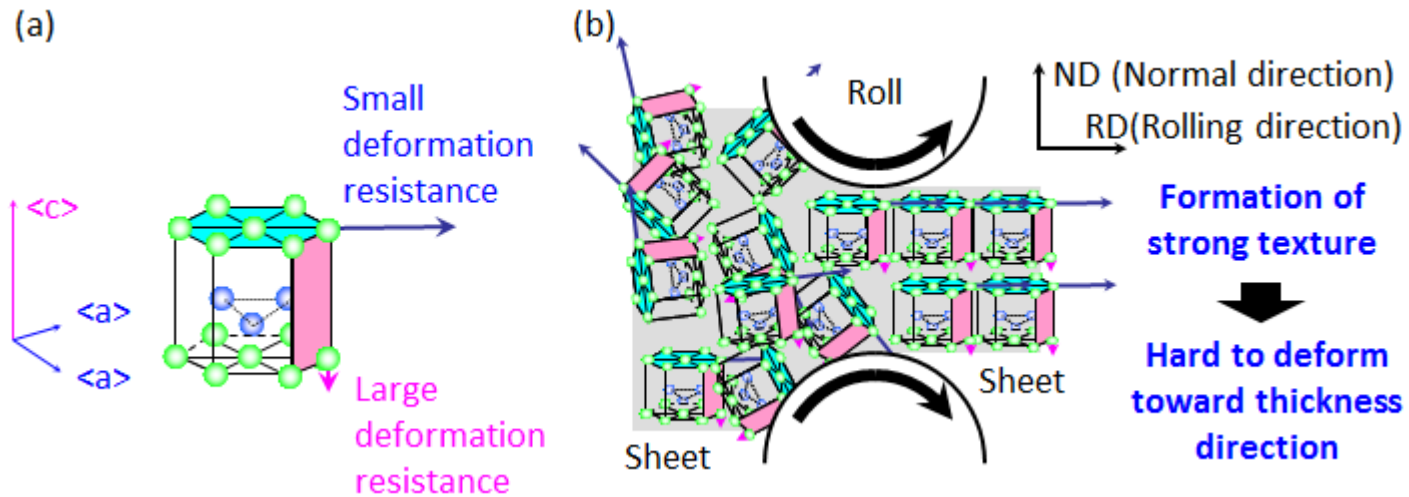
Stamping of metals

Szkic przedstawiający proces głębokiego tłoczenia



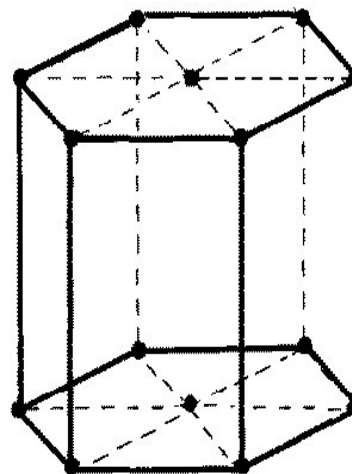
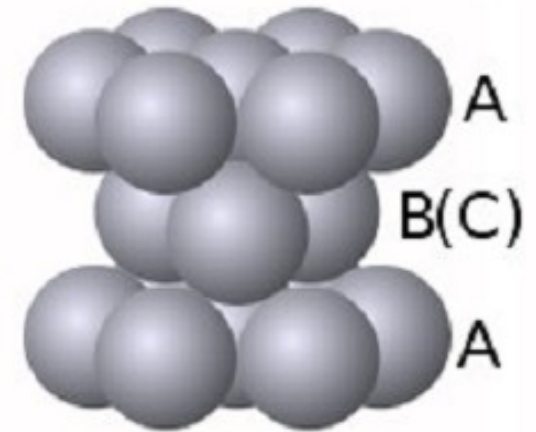
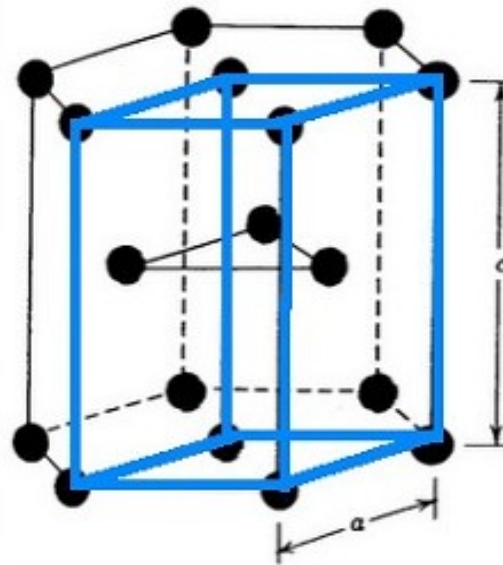


Mechanical anisotropy of hcp metals

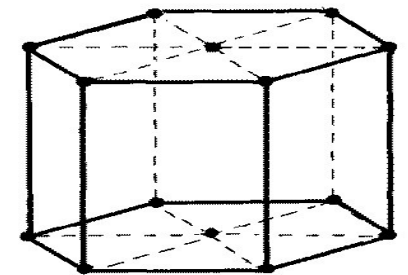


HCP metals

Metal	c/a	a [10^{-10}m]	c [10^{-10}m]	-
Cd	1,8856	2,9788	5,6167	I
Zn	1,8563	2,6649	4,9468	
Co	1,6235	2,507	4,070	
Mg	1,6235	3,2094	5,2109	
Re	1,615	2,760	4,458	II
Tl	1,5984	3,4566	5,5248	
Zr α	1,5931	3,2313	5,1477	
Ti α	1,5873	2,9511	4,6843	
Hf	1,5811	3,1946	5,0511	
Y	1,5712	3,6474	5,7306	
Be	1,568	2,286	3,584	

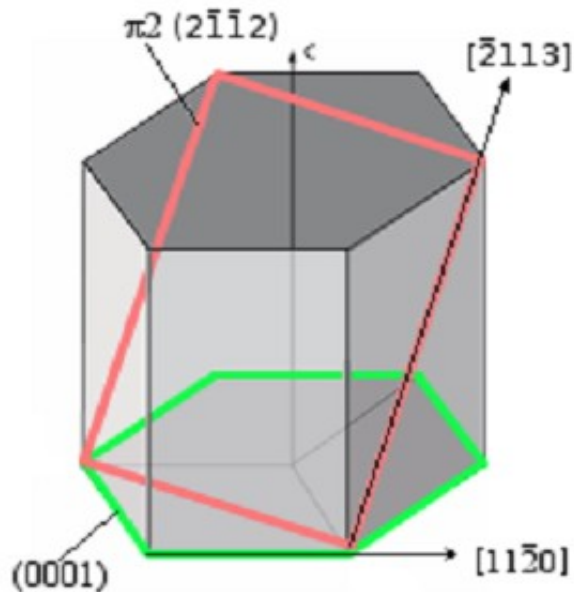


$c/a > 1.633$

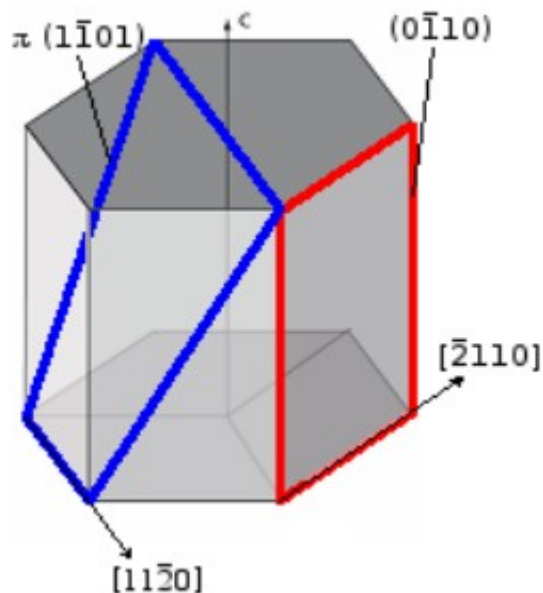


$c/a < 1.633$

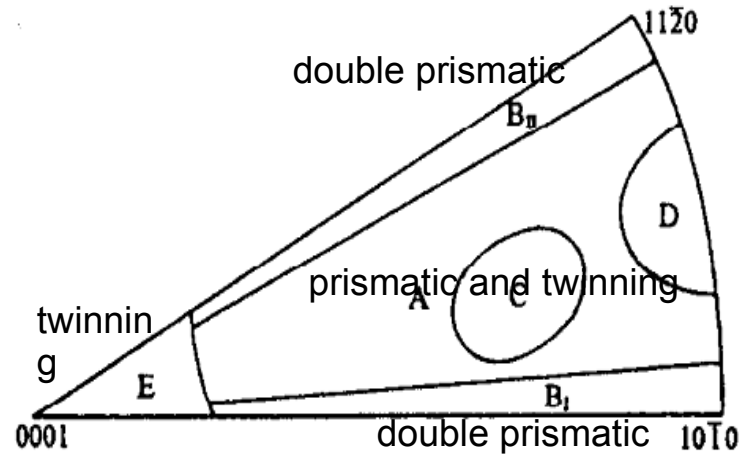
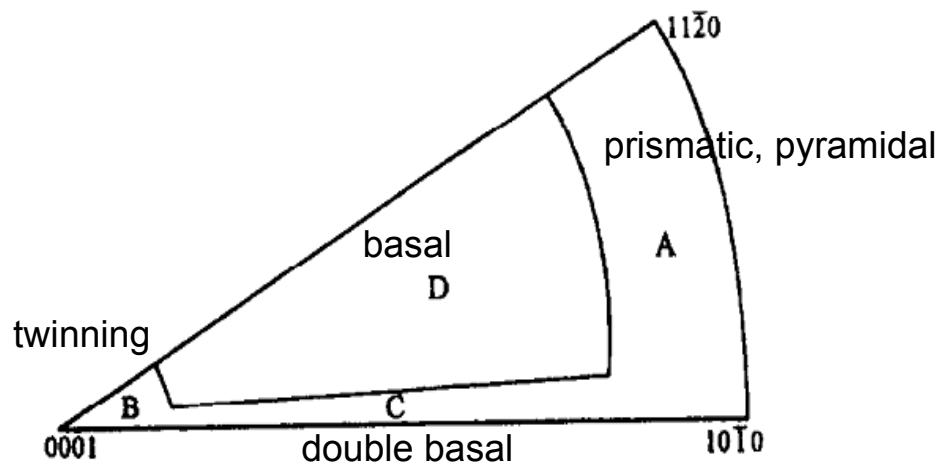
Slip systems in hcp metals



Slip system	Symbol	Plane and direction	Burgers vector	Symbol
Basal	B	$(0001)\langle 11\bar{2}0 \rangle$	$1/3\langle 11\bar{2}0 \rangle$	a
Prismatic	P	$\{10\bar{1}0\} \langle 1\bar{2}10 \rangle$	$1/3\langle 11\bar{2}0 \rangle$	a
Prismatic second order	P_2	$\{11\bar{2}0\}[0001]$	$[0001]$	c
Pyramidal	π	$\{1\bar{1}01\} \langle 11\bar{2}0 \rangle$	$1/3\langle 11\bar{2}0 \rangle$	a
Pyramidal second order	π_2	$\{11\bar{2}2\} \langle 11\bar{2}3 \rangle$	$1/3\langle 11\bar{2}3 \rangle$	$c+a$

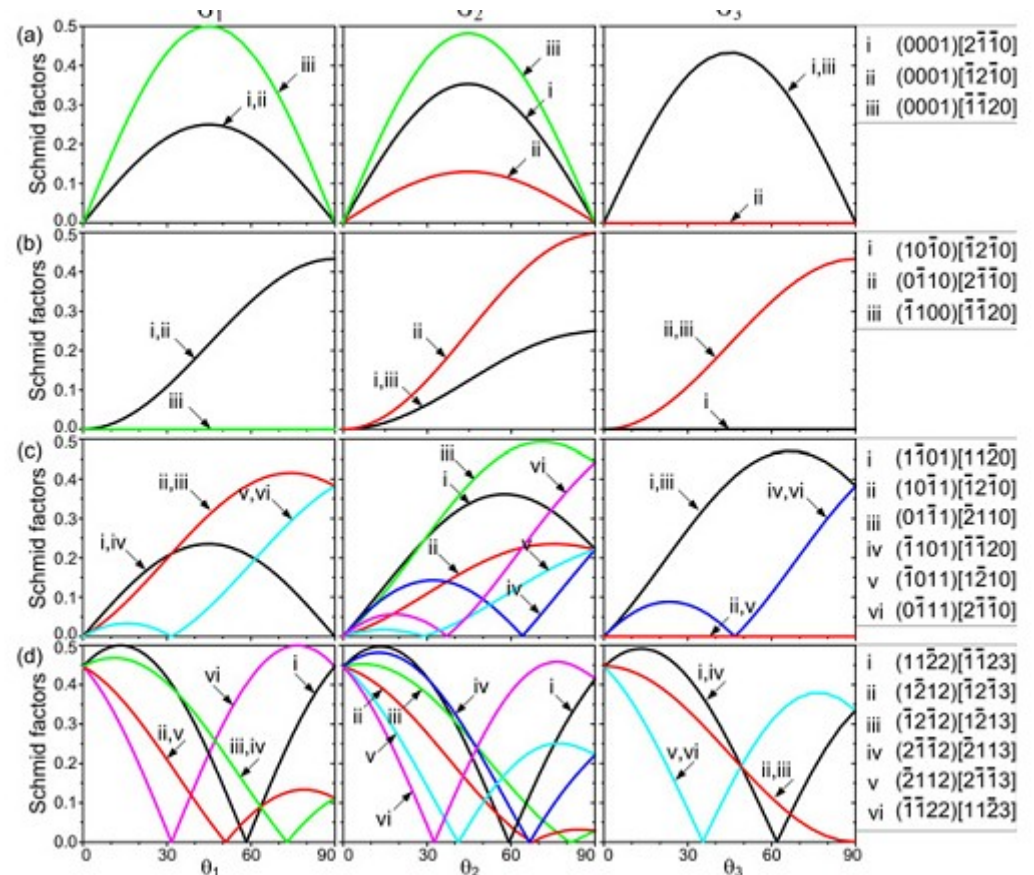
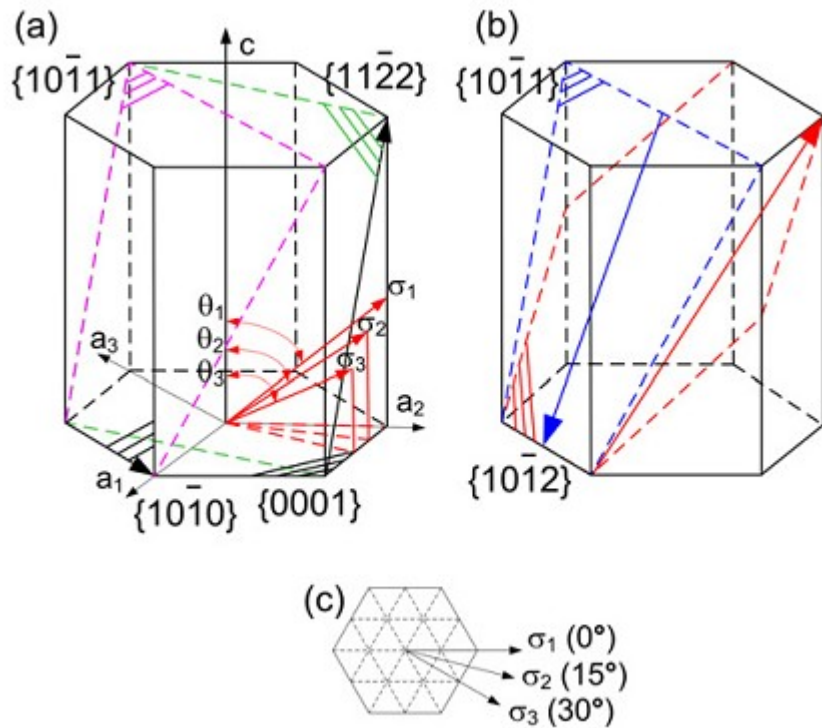


Metal	c/a	Basal $(0001)\langle 11\bar{2}0 \rangle$	Prismatic $\{10\bar{1}0\} \langle 1\bar{2}10 \rangle$	Pyramidal $\{1\bar{1}01\} \langle 11\bar{2}0 \rangle$	Pyramidal 2nd order $\{11\bar{2}2\} \langle 11\bar{2}3 \rangle$
Cd	1,886	$<0,1$	-	~ 7	~ 7
Zn	1,856	$<0,1$	-	-	~ 5
Mg	1,624	$\sim 0,5$	~ 40	-	~ 40
Ti	1,587	~ 80	~ 20	-	-
Be	1,568	~ 5	-	-	-

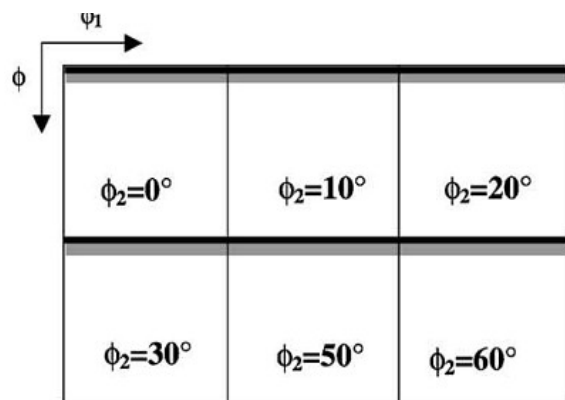
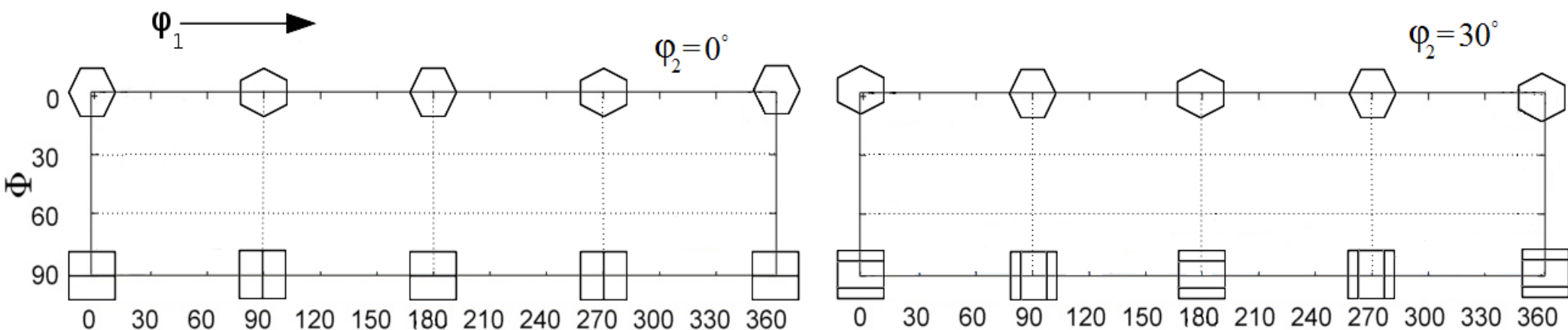


N. Munroe, X. Tan, H. Gu
Scripta Materialia 36, 1383 (1997)

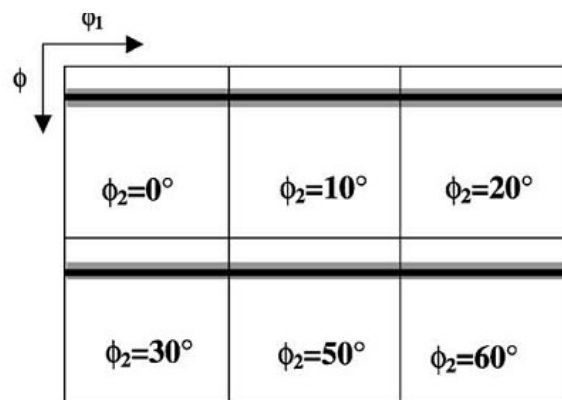
Orientation dependence of plastic deformation in hcp metals: (a) basal slip metals[3]; (b) prismatic slip metals



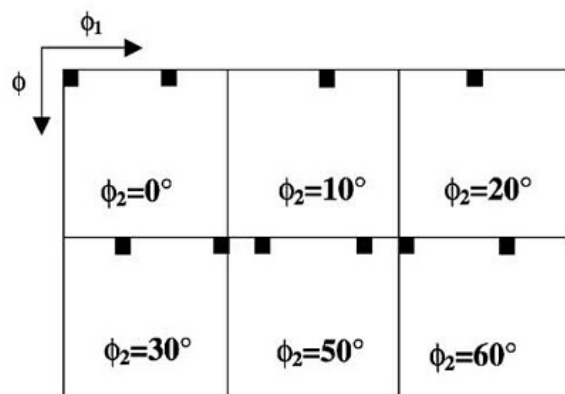
X.L. Nan, H.Y. Wang, L. Zhang, J.B. Li, Q.C Jian, *Scripta Materialia* 67, 443 (2012)



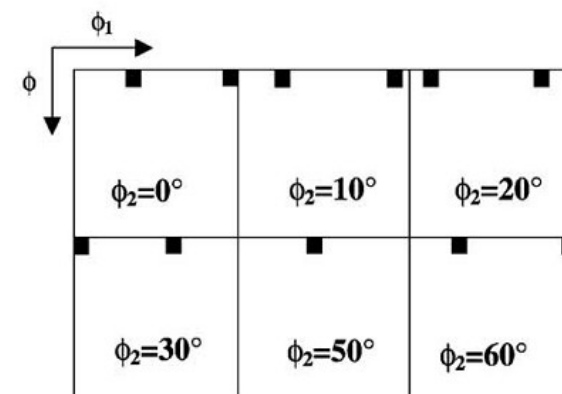
(a) $\{0001\}$ basal fiber



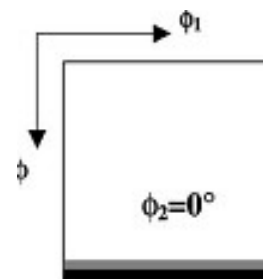
(b) $\{hkil\}$ fiber texture



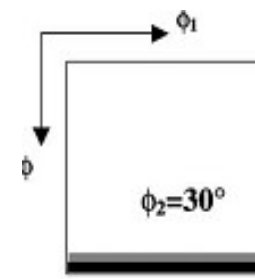
(c) $\{0001\} \langle 10\bar{1}0 \rangle$



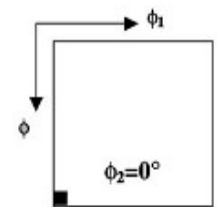
(d) $\{0001\} \langle 11\bar{2}0 \rangle$



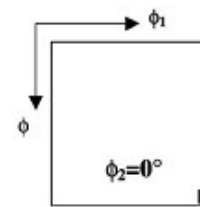
(h) $\{11\bar{2}0\}$ fiber



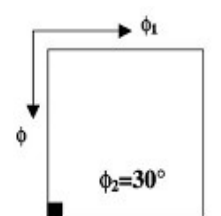
(j) $\{10\bar{1}0\}$ fiber



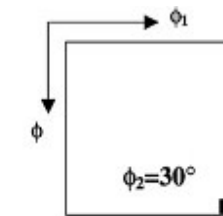
(n) $\{11\bar{2}0\} \langle \bar{1}010 \rangle$



(m) $\{11\bar{2}0\} \langle 0001 \rangle$

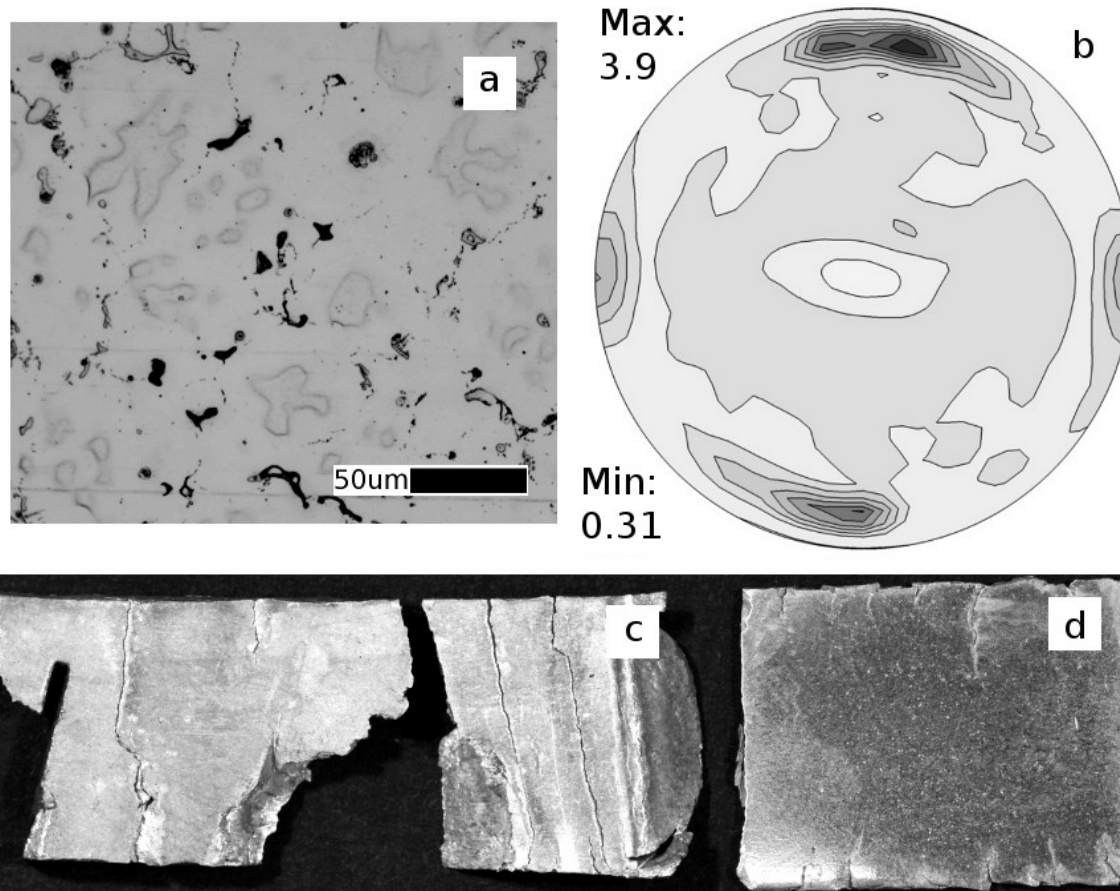


(l) $\{10\bar{1}0\} \langle \bar{2}110 \rangle$



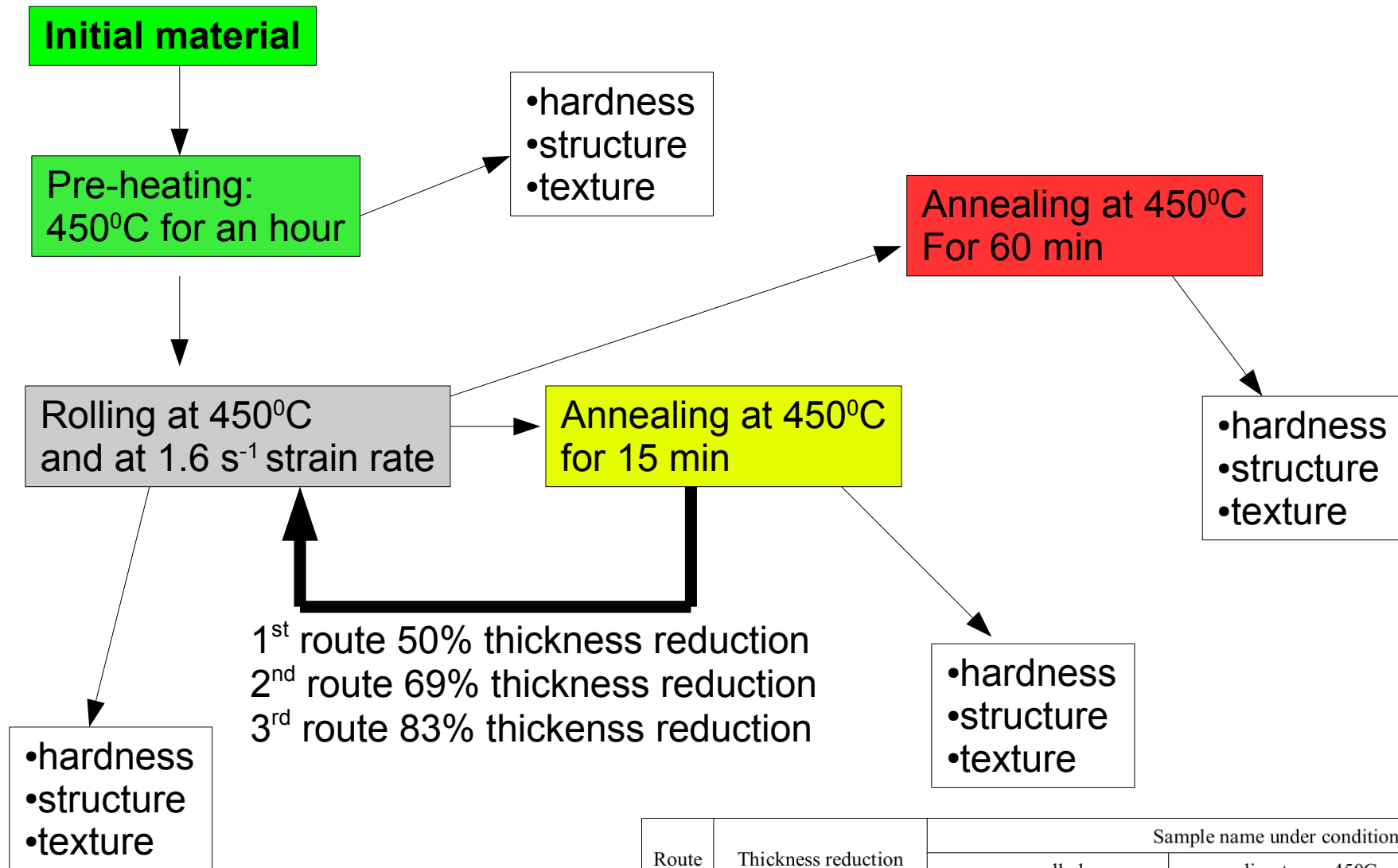
(k) $\{10\bar{1}0\} \langle 0001 \rangle$

Initial sample



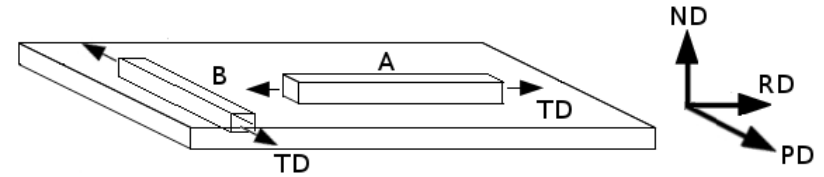
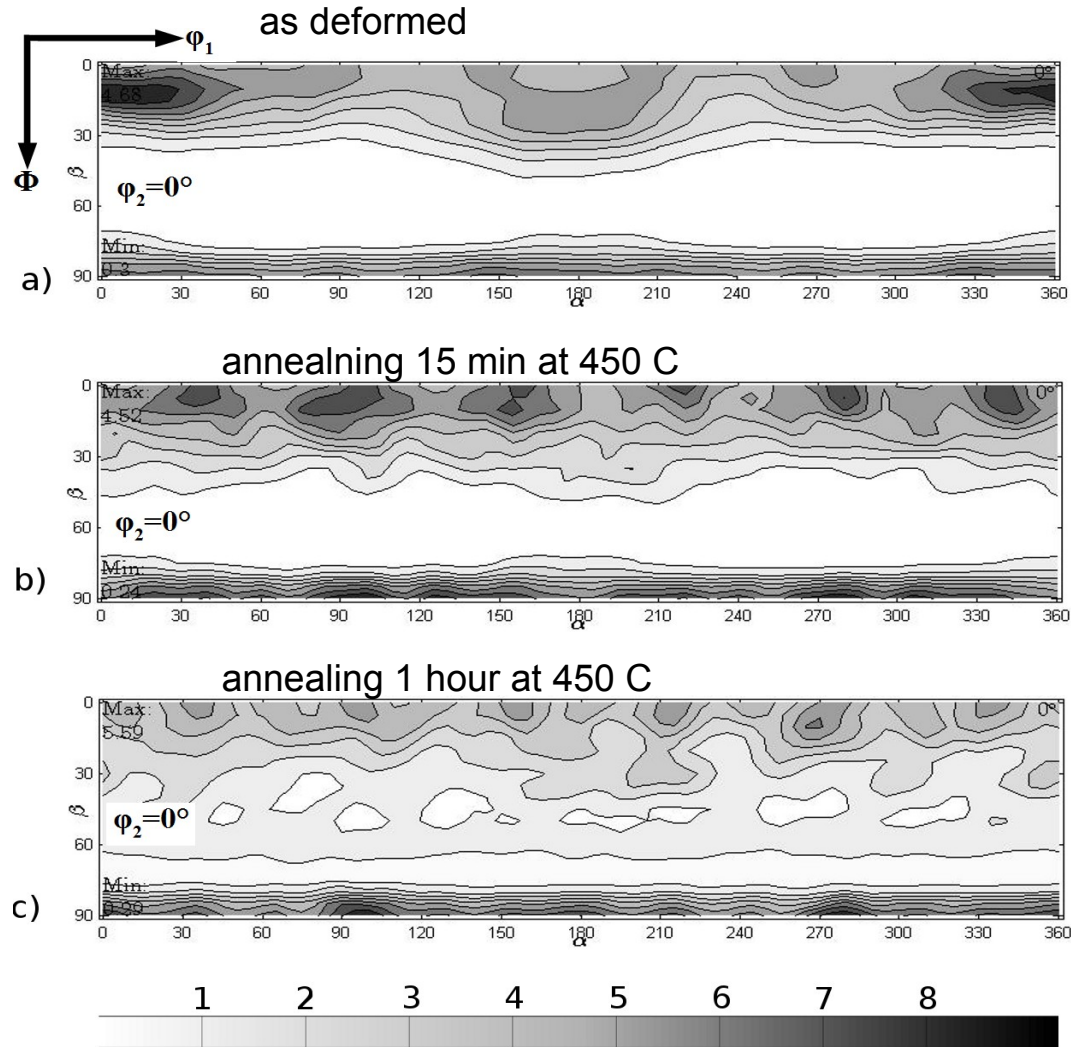
- a) initial structure;
- b) (0002) pole figure after annealing at 450°C and 1 hour before deformation;
- c) sample deformed to 69% of thickness reduction in two passes without annealing;
- d) 3A sample deformed to 83% total thickness reduction in three passes with intermediate annealings.

Hot-rolling and annealing conditions

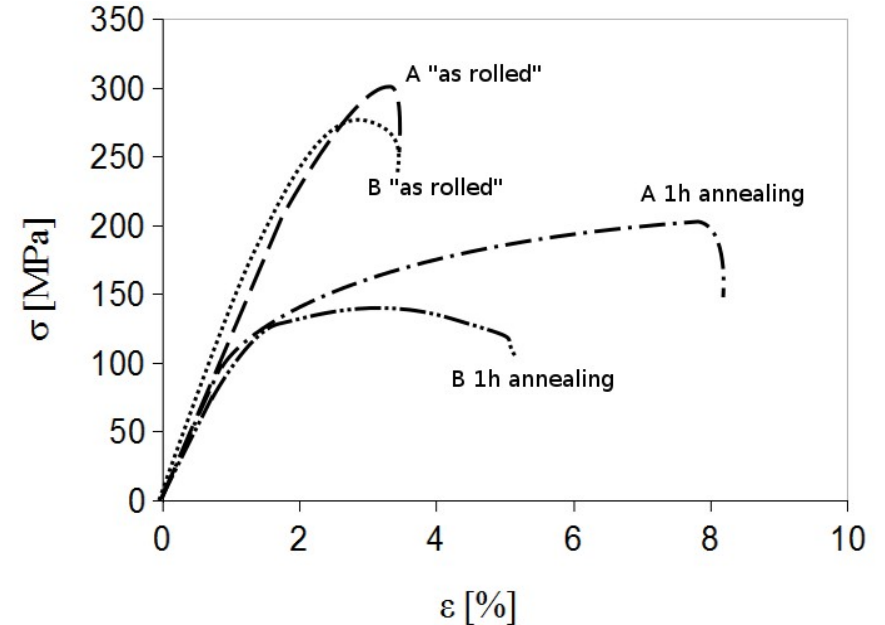


Route	Thickness reduction	Sample name under conditions		
		as-rolled	annealing temp. 450C annealing time = 15 min.	annealing temp. 450C annealing time = 60 min.
0	0	(initial sample)	-	-
1	50%	1A	1B	1C
2	69%	2A	2B	2C
3	83%	3A	3B	3C

ODF $\phi_2 = 0^\circ$ section of AZ61 (a) hot-rolled and (b,c) annealed



The sketch showing samples with TD \parallel RD and TD \perp RD cut for tensile tests



Modeling of texture

Sachs* versus *Taylor

- Diagrams illustrate the difference between the Sachs iso-stress assumption of single slip in each grain (a, c and e) versus the Taylor assumption of iso-strain with multiple slip in each grain (b, d).

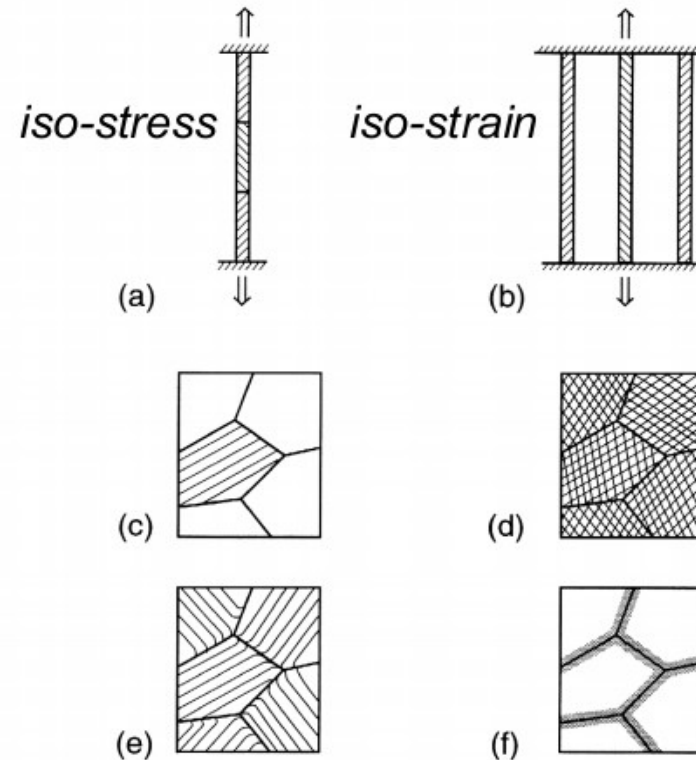


Fig. 23. Schematic description of various polycrystal plasticity models: (a) a true lower bound for a linear serial polycrystal; (b) the Sachs model (independent parallel grains); (c) a true lower bound for a 3-D polycrystal (only one grain deforms at any instant); (d) a true upper bound (also the Taylor model); (e) the Kochendörfer model (single slip plus bending); (f) the Ashby model (polyslip plus 'geometrically necessary dislocations').

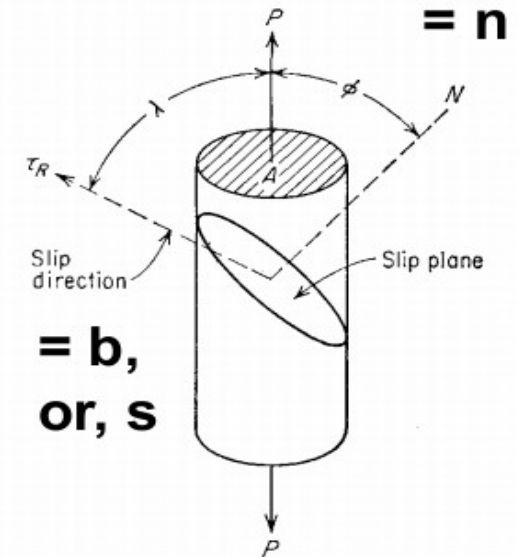
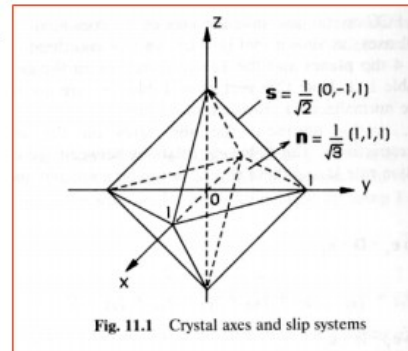
Modeling of texture by Taylor model

- Finding independent five active slip systems

Given : { Slip system - c_3 ; $\dot{\gamma}_{c3}$
 Unit vector in the slip direction - $n = \frac{1}{\sqrt{3}}(-1,1,1)$
 Unit normal vector to the slip plane - $b = \frac{1}{\sqrt{2}}(1,1,0)$

The contribution of the c_3 system is given by

$$\frac{1}{2}(bn + nb)\dot{\gamma}_{c3} = \frac{\dot{\gamma}_{c3}}{2\sqrt{6}} \begin{bmatrix} -2 & 0 & 1 \\ 0 & 2 & 1 \\ 1 & 1 & 0 \end{bmatrix}$$



P is a unit vector in the loading direction

Minimal internal or maximum external work criterion
 (Taylor or Taylor-Bishop method)

$$\sum_{\alpha=1}^n \tau_c \dot{\gamma}_{\alpha} \leq \sum_{\alpha=1}^n \tau_{\alpha}^* \dot{\gamma}_{\alpha}^*$$

$$\dot{\gamma}_s = \dot{\gamma}_0 \left| \frac{\tau_s^r}{\tau_0} \right|^{1/m} \text{sign}(\tau_s^r)$$

$$m_{ij}^{(\alpha)} = b_i^{(\alpha)} n_j^{(\alpha)}$$

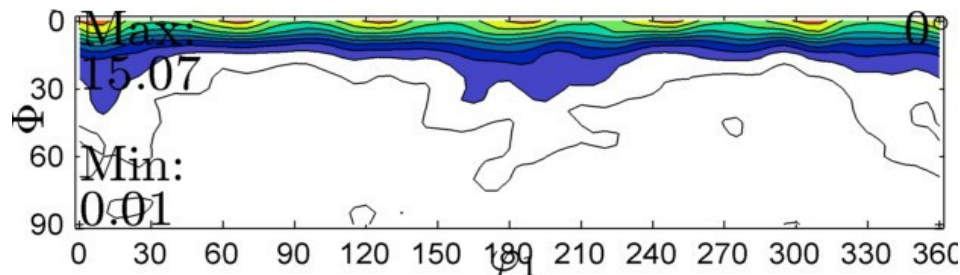
$$d_{ij} = \sum_{s=1}^N M_{ij}^s \dot{\gamma}_s$$

Modeling of texture by Taylor model

- Construct deformation matrix from active slip systems

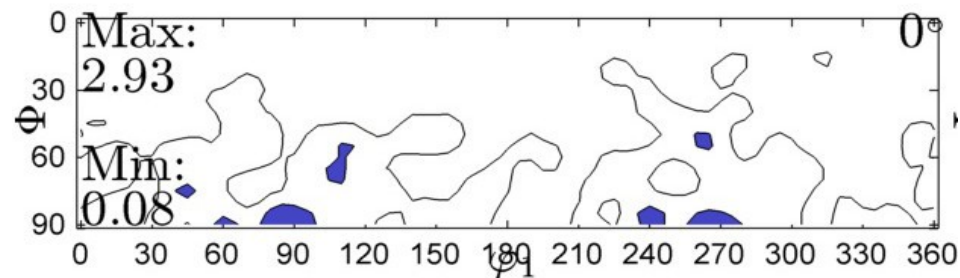
$$D = D^p = \sum_{\alpha=1}^n m_{\alpha} \dot{\gamma}_{\alpha}$$

- Anti-Symmetric part of deformation matrix gives information about change in orientation
- Update actual orientation of grain
- Repeat until last step of deformation



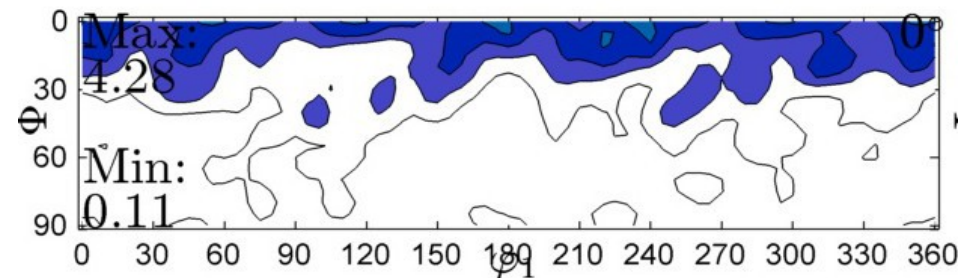
$$\tau_{\text{basal}}/\tau_{\pi 2} = 1/10$$

$$M = 2.8$$



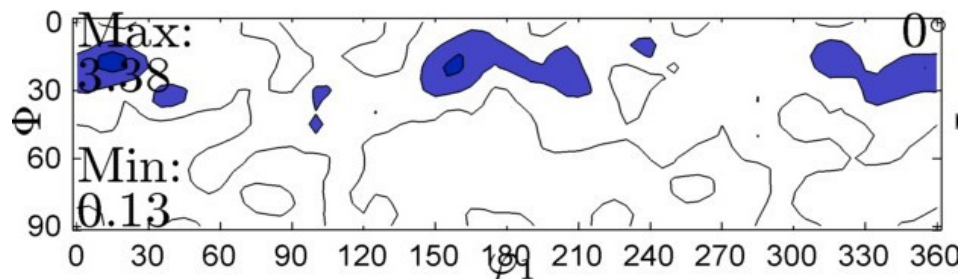
$$\tau_{\text{basal}}/\tau_{\pi 2} = 10/1$$

$$M = 3.5$$



$$\tau_{\text{basal}}/\tau_{\pi 2} = 2/3$$

$$M = 2.1$$



$$\tau_{\text{basal}}/\tau_{\pi 2} = 3/5$$

$$M = 1.4$$

Increase
of temperature



Summary

- AZ61 was deformed by rolling to large thickness reduction at a high strain rate
- After rolling the texture is of basal type with $[0001]$ split into two peaks toward RD
- During intermediate annealing $\{11\bar{2}0\} \langle 10\bar{1}0 \rangle$ component of texture is strengthened
- Twins which form during rolling may support the texture changes during static annealing
- Texture changes have an impact on enhancing the ductility of AZ61

Thank you for your attention